

# A Novel Solar and Electromagnetic Energy Harvesting System with a 3D Printed Package for Energy Efficient Internet-of-Things (IoT) Wireless Sensors

Jo Bito\*, *Student Member, IEEE*, Ryan Bahr\*, *Student Member, IEEE*, Jimmy G. Hester\*, *Student Member, IEEE*, Syed A. Nauroze\*, *Student Member, IEEE*, Apostolos Georgiadis<sup>†</sup>, *Senior Member, IEEE*, and Manos M. Tentzeris\*, *Fellow, IEEE*,  
(Invited Paper)

**Abstract**—This paper discusses the design of a novel dual (solar+electromagnetic) energy harvesting powered communication system, which operates at 2.4 GHz ISM band, enabling the autonomous operation of a low power consumption power management circuit for a wireless sensor, while featuring a very good “cold start” capability. The proposed harvester consists of a dual port rectangular slot antenna, a 3D printed package, a solar cell, an RF-dc converter, a power management unit, a micro-controller unit, and an RF transceiver. Each designed component was characterized through simulation and measurements. As a result, the antenna exhibited a performance satisfying the design goals in the frequency range of 2.4 to 2.5 GHz. Similarly, the designed miniaturized RF-dc conversion circuit generated a sufficient voltage and power to support the autonomous operation of the bq25504 power management unit for RF input power levels as low as -12.6 dBm and -15.6 dBm at the “cold start” and “hot start” condition, respectively. The experimental testing of the power management unit utilizing the proposed hybrid energy harvester confirmed the reduction of the capacitor charging time by 40% and the reduction of the minimum required RF input power level by 50% compared with the one required for the individual RF and solar harvester under the room light irradiation condition of 334 lx.

**Index Terms**—Energy harvesting, RF circuits, solar cell, rectennas, 3D printing, additive manufacturing, Internet-of-Things, wireless sensors, hybrid system, power management, autonomous RF system

## I. INTRODUCTION

**N**OW-A-DAYS, the desire for a smart society that utilizes technologies such as large-scale sensor networks [1], the Internet of Things (IoT) [2], and smart skins [3], [4] is continuously growing. One of the most pressing issues is the lack of a sustainable power supply that could enable the autonomous operation of these sensors and devices (motes). Conventional autonomous devices heavily rely on primary batteries, which can power the devices for only a certain amount

of time. Once the sensor devices use up the stored energy in their batteries, the batteries need a replacement at a cost that increases significantly as the number of sensor devices in the system increases. To avoid this maintenance cost issue and achieve completely self-sustainable low-cost ubiquitous systems for the IoT and smart cities, research communities have devoted a considerable interest in ambient energy harvesting technologies. To maintain an effective operation of truly autonomous systems, this technology set harnesses energy from numerous ambient power sources such as solar, heat, vibration, and electromagnetic waves using transducers and stores it in energy storage components such as secondary batteries and capacitors [5]–[7]. Among the ambient energy sources, radio frequency (RF) energy is a highly attractive energy source because of its almost ubiquitous availability, especially in urban areas as well as the low cost and size of transducers [8], [9]. However, compared to the energy density of other energy sources, that of RF energy is typically very low [5]. Therefore, RF energy harvesters cannot directly drive devices that require relatively high power and voltage such as micro-controllers, especially from a “cold start” condition. Since low energy density levels cause a low RF-dc conversion efficiency, RF energy harvesting is even more challenging to be practically exploited [10]–[12].

### A. Additive manufacturing techniques for ambient energy harvesting modules

To overcome the low-energy-density problem in RF energy harvesting, researchers have strived in the last several decades to improve the performance of RF energy harvesters. In the process, additive manufacturing technology has emerged as an alternative to conventional fabrication techniques such as etching and milling [13]–[15]. Specifically, additive manufacturing technology including inkjet printing, 3D printing, and screen printing has proven to be a very efficient solution for low-cost RF circuit patterning associated with an inherently high 2D/3D resolution and a wide variety of printable materials [16]. In the field of electrical engineering, the inkjet-printing technology has already enabled the easy realization of high-resolution conductive traces that can support the operation of circuits up to the sub-terahertz frequency range on a variety of substrates including flexible materials such as paper, plastic, and liquid crystal polymer (LCP) [17], [18]. In addition to conductive materials, various dielectric materials and semi-conductive materials can be printed using inkjet-printing technology, which

The work of J. Bito, R. Bahr, J.G. Hester, S.A. Nauroze, and M.M. Tentzeris was supported by national science foundation emerging frontiers in research and innovation (NSF-EFRI), defense threat reduction agency (DTRA), semiconductor research corporation (SRC), and Texas Instruments.

\*J. Bito, R. Bahr, J.G. Hester, S.A. Nauroze, and M.M. Tentzeris are with the School of Electrical and Computer Engineering, Georgia Institute of Technology, Atlanta, GA, 30332-250, USA, (e-mail: jbito3@gatech.edu).

The work of A. Georgiadis was supported under EU H2020 Marie Skłodowska-Curie Grant Agreement 661621.

A. Georgiadis would also like to acknowledge EU COST Action IC1301 Wireless Power Transmission for Sustainable Electronics.

<sup>†</sup>A. Georgiadis is with Heriot-Watt University, Institute of Sensors, Signals and Systems, Edinburgh EH14 4AS, UK, (email: a.georgiadis@hw.ac.uk)

allows for the full printing of most basic circuit components such as capacitors, inductors, antennas, diodes, and so on [19]–[21]. Another additive manufacturing technique, which has recently attracted the attention of the research community, is 3D printing, especially the fused deposition modeling (FDM) technology [22], [23]. The wide variety of printable materials for these additive manufacturing techniques has also enabled the easy fabrication of both transducers and energy storage components for ambient harvesting from most energy sources.

### B. Multi-energy source hybrid energy harvesting

Numerous renewable ambient energy sources, such as solar, heat, vibration, and electromagnetic waves, exist in nature. Each ambient energy source exhibits different characteristics, and they all have both advantages and disadvantages. In reality, when autonomous systems completely rely on ambient energy sources, the major challenges associated with harvesting a single source of energy can cause critical issues for device operation. For example, an autonomous system relying exclusively on the energy harvested by a photovoltaic panel (e.g. a solar panel) will fail in the absence of light. Instead of relying on a single source, energy harvesting of multiple sources can be complementary and enable truly autonomous operation, as mentioned in [5]. Among various ambient energy sources, solar energy has been one of the most commonly sought-after because of the large power density available for harvesting during the daytime (ca.  $100 \text{ mW} \cdot \text{cm}^{-2}$ ). Niotaki et al. have reported on a hybrid RF/solar energy harvester, which can significantly increase the total available power available in a system [24]. As another example, Georgiadis et. al and De Denno et al. have demonstrated a hybrid solar/EM energy harvesting system which extends the operation range of a passive RFID tag [25], [26]. The power conversion efficiency of electromagnetic energy contained in the solar spectrum to electricity depends on the level of illumination, the photoactive material and device architecture used. At low irradiance levels, like the ones found indoors (ca.  $100 \mu\text{W} \cdot \text{cm}^{-2}$ ), the performance of a photovoltaic device becomes limited by increased power losses that arise as the value of the devices shunt resistance becomes comparable to that of the characteristic resistance of the cell; defined as the ratio between the open circuit voltage and the short-circuit current. Among current photovoltaic technologies, those based on organic semiconductors shown in [27], [28] are particularly suitable for low-light level operation. In addition, organic photovoltaic devices are compatible with all-additive manufacturing methods such as ink-jet printing [29] and are therefore attractive for integration with RF energy harvesting modules to increase the available power per unit area [30]–[32].

### C. Challenges in ambient RF energy harvesting

Regardless of the typically low energy density of ambient RF, RF energy harvesting is an attractive research topic for various reasons. First, RF energy can inherently penetrate most walls, even opaque walls, so it is potentially more widespread available than other ambient energy sources. In addition, RF energy harvesters can operate at any time of the day and

with any topology. Finally, their miniaturized form factor, their small physical dimensions, and light weight enable us to easily carry or wear them. On the other hand, the typically low ambient RF energy density can be highly problematic, especially when the RF energy harvester is integrated with entirely autonomous systems because of their minimum input power and voltage requirements. As a general trend, Schottky diodes have been mainly used for RF energy harvesting because of their low threshold voltage and fast switching speed. However, Hemour et al. [33] have reported that the performance of off-the-shelf Schottky diodes are reaching the maximum theoretical RF-dc conversion efficiency because of inevitable series resistance, junction capacitance, and high junction resistance associated with their operation principle, especially with low RF input power. Therefore, several studies have recently applied special types of diodes such as the backward tunnel (Esaki) diodes and the metal-insulator-metal (MIM) diodes to rectify extremely low RF input power of below  $1 \mu\text{W}$  [33], [34]. Another strategy is to maximize the available RF input power using multi-band frequencies by introducing an ultra wide band (UWB)/ multi-band antenna and a wide band matching circuit topology in the rectenna [8], [35]–[37].

Recently, sub-threshold operation of a switching transistor has been studied actively and it has been proven that some transistors can operate even below  $0.4 \text{ V}$  in the field of research [38], [39]. However, most off-the-shelf circuit components require relatively high operation voltage. For example, a typical transistor gate-source voltage requires at least  $0.5 \text{ V}$  for switching operation and ICs such as micro-controllers require an even higher operation voltage above  $1.5 \text{ V}$  [12], [40], [41], whereas typical voltages from the rectifier with RF input power under  $-20 \text{ dBm}$  are below  $0.3 \text{ V}$  [42]. To overcome this low-voltage issue, researchers have developed dc-dc converters with low input voltage operation capabilities. Carlson et al. [43] reported a dc-dc boost converter that generates the output voltage of  $1 \text{ V}$  from the input voltage as low as  $20 \text{ mV}$ , with the power consumption of  $1.6 \mu\text{W}$ . However, the voltage regulator requires at least  $0.6 \text{ V}$  of start up voltage in a capacitor to initially start the operation of the circuit oscillators. Another example is a self-powered dc-dc converter reported by Adami [44], which can generate the output voltage of  $1 \text{ V}$  from an input voltage close to  $100 \text{ mV}$  without any external power supply, but it requires at least  $10 \mu\text{W}$  of input dc power and reported dc-dc conversion efficiency is below  $25 \%$  because of inevitable power loss associated with the self-oscillation. To satisfy both of these power and voltage requirements, reported RF power sensitivity is  $-13 \text{ dBm}$  for  $1 \text{ V}$  and  $-7 \text{ dBm}$  for  $3 \text{ V}$  of output voltage. These facts imply that adding solar cells, which generate a nearly constant voltage under sufficient illumination conditions can enable the “cold start” start-up operation of a dc-dc converter allowing RF energy harvesters to then scavenge low power energy. At the same time, RF energy harvesters continuously generate energy during the night time when solar cells cannot generate any power.

To sufficiently address the main challenges of RF energy harvesting, by taking advantage of the unique features of additive manufacturing, one possible solution is the combination

of multiple source ambient energy harvesting. In particular, this research proposes the hybridization of RF and solar energy harvesters in modules/topologies that can be fabricated utilizing additive manufacturing technology. The following sections of the paper deal with an overview of the proposed hybrid RF solar energy harvesting system, the design and preliminary measurements of the antenna and the rectifier, the preliminary module-level operation results and the hybrid harvester benchmarking in comparison to previously reported RF/solar energy harvesters, while the paper closes with the conclusions.

## II. HYBRID RF SOLAR ENERGY HARVESTING SYSTEM

As a proof-of-concept prototype that can be easily implemented in a compact form factor, this research utilized a TI bq25504 ultra low power boost converter with battery management IC, which has a self-powered dc-dc converter for “cold start” operation and a high efficiency dc-dc converter with maximum power point tracking for “hot start” operation [45]. Fig. 1 shows the block diagram of an autonomous hybrid RF solar powered sensor device (mote). The device consists of a dual port antenna both for harvesting and communication at the 2.4 GHz ISM band, a solar cell, a matching circuit, an RF-dc conversion circuit, a bq25504 power management unit (PMU), a capacitor/battery for energy storage, a MOSFET switch, an MSP430 micro-controller unit (MCU) [41], and a CC2500 transceiver for communications [46].

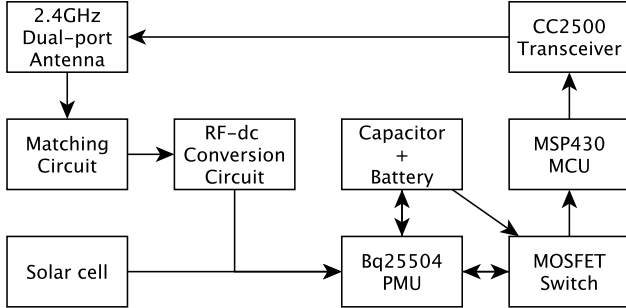


Fig. 1. Block diagram of a hybrid RF solar powered autonomous mote.

## III. ANTENNA DESIGN AND MEASUREMENT

This proposed system uses the 2.4 GHz ISM band for both energy harvesting and communications. Therefore, the antenna requires a dual port configuration with a high two-port isolation. In addition, circular polarization is suitable for RF energy harvesting as it allows the rectenna to capture signals with arbitrary linear polarization. In this scenario, a properly excited rectangular shorted slot antenna [47], [48] was identified as a strong candidate which also exhibits a good impedance and polarization bandwidth. The biggest novelty and challenge in designing the antenna for our energy harvesting capable mote is to feature a simultaneous two-port operation; one port for energy harvesting and another port for communication while sharing the same rectangular slot. The design and location of the feeding transmission

lines as well as the size and height of the ground plane are critical to realize a good matching for both ports and a simultaneous high isolation between the two ports. Since the rectangular shorted slot antenna is an omnidirectional antenna, a reflector was placed on the bottom of the package in order to increase the gain. The package was printed utilizing a 3D printer to precisely control the distance between the ground of the antenna and the reflector. The antenna was designed utilizing HFSS and fabricated on a 0.762 mm FR4 substrate with dielectric constant of 4.4 and loss tangent of 0.002 utilizing an LPKF ProtoMat S60 mechanical milling machine. Fig. 2 shows the side and top view of the rectangular shorted antenna and Table I summarizes the antenna design parameters. In this research, port1 is for harvesting and port2 is for communication. Fig. 3 shows the pictures of the prototype of the solar antenna, i.e., an antenna with an embedded solar cell. The package was created utilizing a fused deposition modeling (FDM) printer with polylactic acid (PLA) based-material. For an initial simulation, the dielectric constant of 3.1 and the loss tangent of 0.01 [49] were adopted. However, Meriakri et al. [50] have reported a wide variation of dielectric constant of PLA material (2.76 to 15.7) which can cause a shift in the fabricated antenna operation frequency.

The design goals of the antenna are the following: (1)  $S_{11}$  and  $S_{22}$  below  $-13$  dB (5%), (2)  $S_{21}$  below  $-13$  dB (5%), and (3) axial ratio below 3 dB in the frequency range of 2.4 to 2.5 GHz. To satisfy these design goals, the length ( $L$ ) of the sides of the square slot and the length of the gap ( $G$ ) were determined to obtain a resonance at 2.45 GHz. In terms of impedance matching, the length and the width of the feeding signal lines can be adjusted to control the center frequency of operation. In addition, the proposed antenna design can adjust the center frequency of the two-port isolation (the peak of transmission loss) almost independently from the matching condition by varying the length of the square side of the ground plane ( $L_{in}$ ). As illustrated in Fig. 4, preliminary simulations varied  $L_{in}$  from 42 to 48 mm, while a value of 45 mm was adopted for the initial antenna prototype. Fig. 5 (a) depicts the simulated (design and post fabrication) and measured  $S_{11}$  and  $S_{22}$ , respectively. From the measurement, the antenna features the operation range of 2.28 to 2.55 GHz, and the simulation results match well with the measurement results. However, as depicted in Fig. 5 (b), the frequency at the peak of transmission loss ( $|S_{21}|$ ) was shifted to lower frequency. During the fabrication, an extra PLA layer with the thickness of 0.5 mm was added below the top PCB as a mechanical support of the antenna structure preventing the top PCB from dropping in the middle of the box. This extra thickness ( $T_{PE}$ ) was taken into account in the post-fabrication simulation model. Also, as mentioned above, the dielectric constant of the PLA material for the package can be higher than the value used in the initial simulation. Therefore, the post-fabrication simulation adopted the dielectric constant of 4, and the simulation exhibited a good agreement with the measurement. This fact implies that further accurate simulations for the antenna design require the accurate characterization of the 3D printed PLA material. Over all, the measured  $S$ -parameters satisfied the design goals (1) and (2).

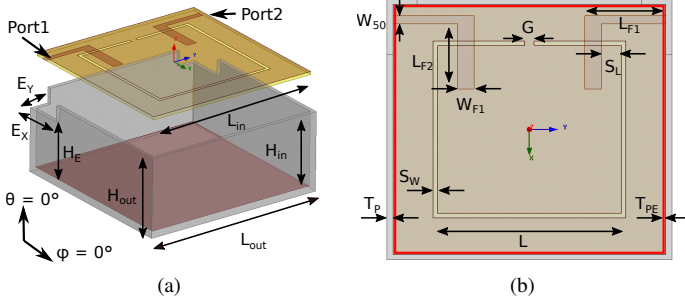


Fig. 2. (a) Side and (b) top view of the prototype of the rectangular shorted antenna.

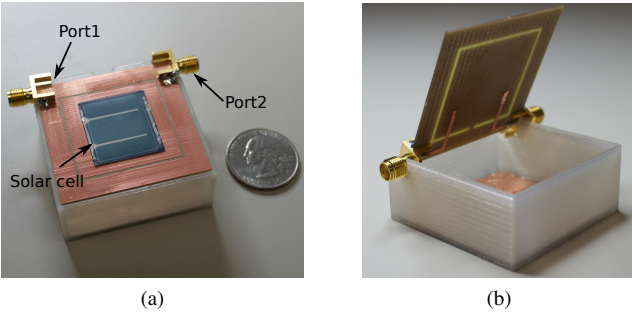


Fig. 3. Prototype of the dual-feed rectangular shorted slot solar antenna with a flexible film solar cell (a) top and (b) inside.

TABLE I  
PRELIMINARY DIMENSIONS OF THE DUAL-FED  
RECTANGULAR SHORTED ANTENNA.

Parameter	$H_{in}$	$H_{out}$	$H_E$	$L_{in}$	$L_{out}$	$E_X$	$E_Y$
Length (mm)	18	20	14	45	47	10	5
Parameter	$L_{F1}$	$L_{F2}$	$L$	$W_{F1}$	$W_{50}$	$S_W$	$S_L$
Length (mm)	13.35	7	11.81	31	1.46	0.9	3.1
Parameter	$G$	$T_P$	$T_{PE}$				
Length (mm)	1.6	1	0.5				

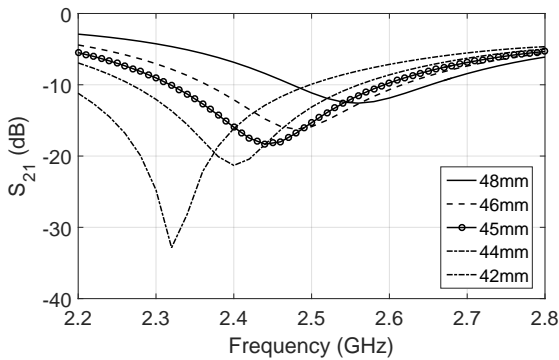


Fig. 4. Simulated  $S_{21}$  with respect to frequency with varied ground size.

In addition to the S-parameters, this study characterized the other properties of the antenna through simulations and measurements. Fig. 6 (a) and (b) show the simulated axial ratio with respect to frequency at broadside ( $\theta = 0^\circ$ ) and  $\theta$  direction rotation angle at 2.45 GHz, respectively. The axial ratio is about 3 dB in the frequency range of 2.4 to 2.5 GHz, which almost satisfies the design goal (3). Also, Fig. 7

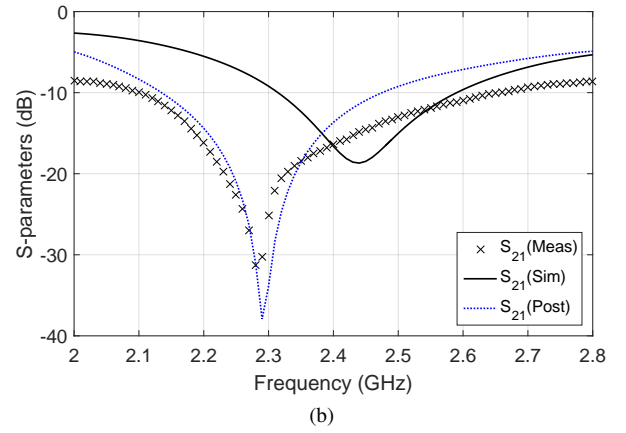
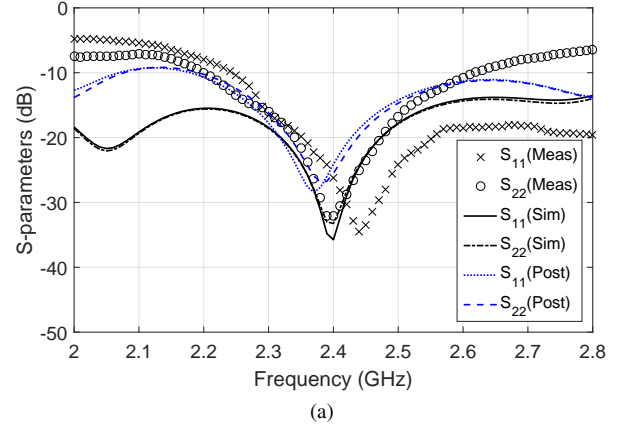
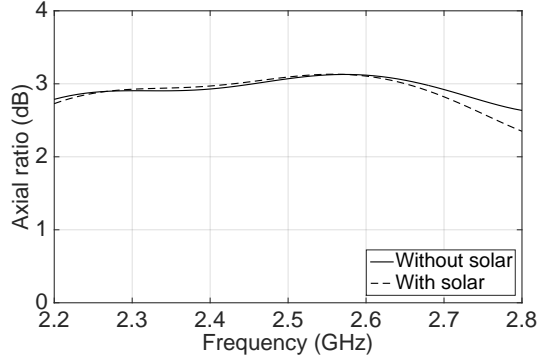
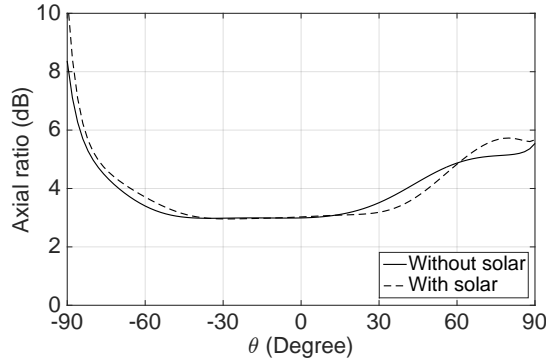


Fig. 5. Measured and simulated (design and post fabrication) (a)  $S_{11}$ ,  $S_{22}$ , and (b)  $S_{21}$  of the dual-feed rectangular shorted slot antenna.

which plots simulated total realized gain as a function of frequency yielding a value of 7.4 dB at the center frequency of 2.45 GHz. For the final prototype, a thin film solar cell, which Section IV explains the detail, is placed on top of the conductive area inside the slot without significantly disturbing its radiation characteristics. Therefore, the radiation patterns, depicted in Fig. 8, were also measured utilizing a LabVIEW controlled automatic rotation setup and a vector network analyzer (Anritsu 37369d). The measurement utilized a broadband horn antenna (AINFO LB-20245) as a reference. The measurements depicted on Fig. 8 show that the solar cell does not have a significant effect on the performance of the dual-feed rectangular antenna. Fig. 9 shows the side and the top view of the rectangular shorted antenna for the final prototype and Table II summarizes the final antenna design parameters. For simplicity in measurements, SMA connectors were connected to the edges of the antenna, but the final prototype of the sensor device (mote) was designed to have all electronics connected to the antenna on the bottom layer near the center of the rectangular slot. Therefore, as shown in Fig. 9 the design of the excitation lines were modified for the final prototype. Fig. 10 shows the simulated S-parameters of the final antenna design.



(a)



(b)

Fig. 6. Simulated axial ratio of the rectangular shorted antenna with and without the solar cell with respect to (a) frequency and (b)  $\theta$  direction rotation angle.

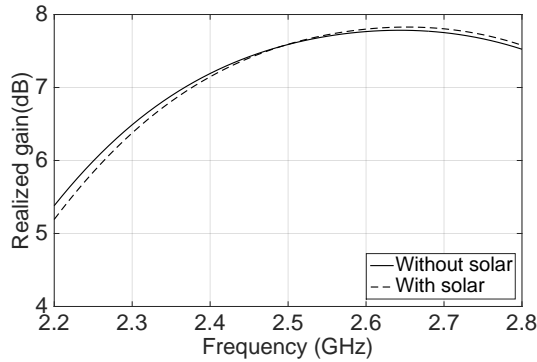


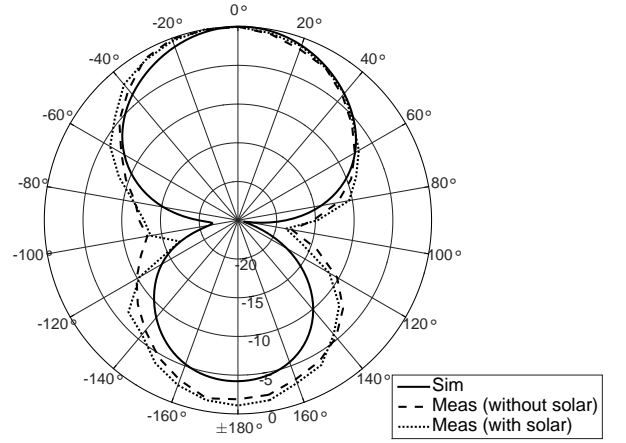
Fig. 7. Simulated total realized gain of the rectangular shorted antenna with and without the solar cell.

TABLE II  
DIMENSION OF THE RECTANGULAR SHORTED ANTENNA  
FOR THE FINAL PROTOTYPE.

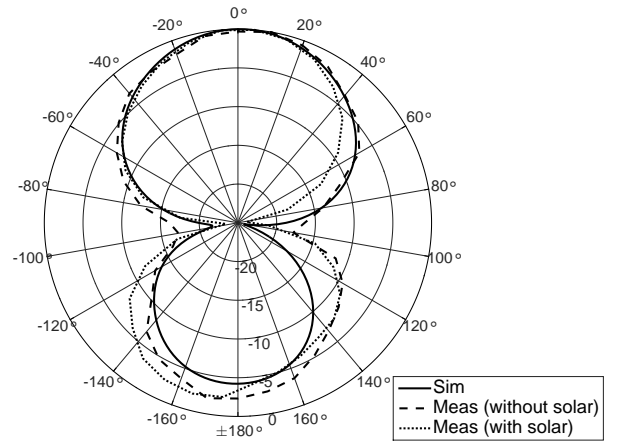
Parameter	$H_{in}$	$H_{out}$	$L_{in}$	$L_{out}$	$L_{F1}$	$L_{F2}$	$L$
Length (mm)	18	20	45	47	13.5	10	31
Parameter	$W_{F1}$	$W_{F2}$	$W_{50}$	$S_W$	$S_L$	$T_P$	$G$
Length (mm)	4	7	1.46	0.9	4.6	1	1.6

#### IV. RF-DC CONVERSION CIRCUIT DESIGN AND MEASUREMENT

The solar cell selected for the proof-of-concept prototype was the Power Film MP3-25 solar cell which has the dimen-



(a)



(b)

Fig. 8. Measured and simulated normalized radiation pattern of the rectangular shorted antenna with and without the solar cell (a)  $\phi = 0^\circ$  and (b)  $\phi = 90^\circ$ .

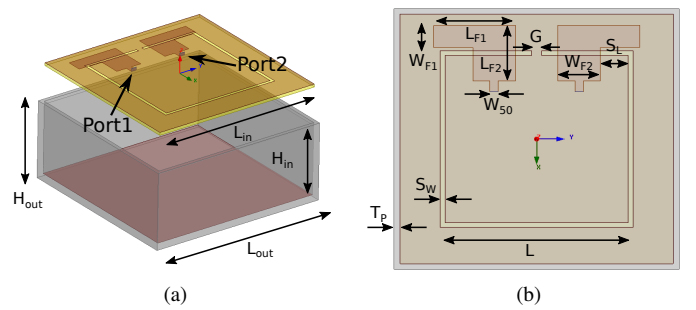


Fig. 9. (a) Side and (b) top view of the rectangular shorted antenna for the final prototype.

sions of 114 mm x 24 mm, short circuit current  $I_{sc} = 48$  mA, open circuit voltage  $V_{oc} = 4.1$  V, and can provide up to 93 mW at 3 V under 1 sun irradiance of  $100 \text{ mW} \cdot \text{cm}^{-2}$ . Specifically for the 3D printed prototype discussed in this paper, only one fifth of the length of the solar module, which exhibits about 0.68 V of open voltage and about  $70.5 \mu\text{W}$  of maximum power under a room light condition ( $334 \text{ lx} = 49 \mu\text{W} \cdot \text{cm}^{-2}$ ) with a dc load resistance of  $3.8 \text{ k}\Omega$ , was utilized in order to fit within the conductive surface inside the dual-fed slot antenna,

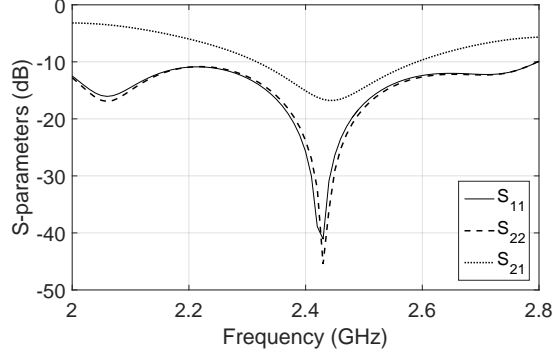
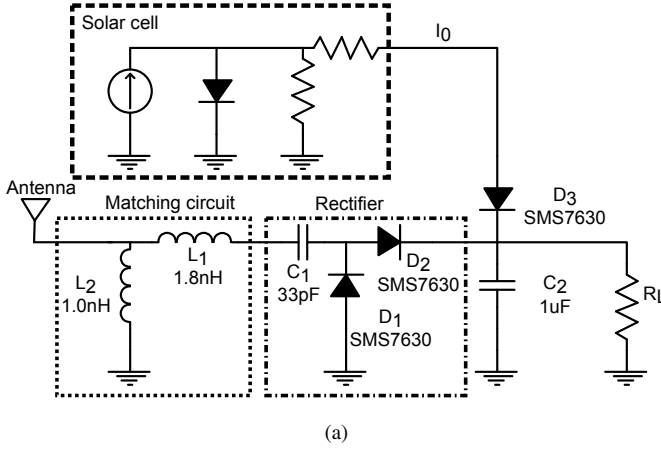
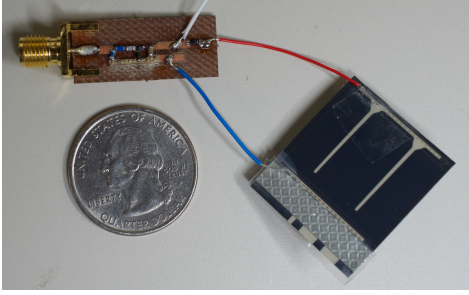


Fig. 10. Simulated S-parameters of the final antenna design with respect to frequency.



(a)

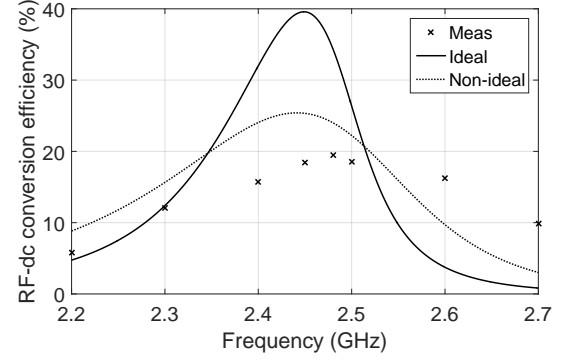


(b)

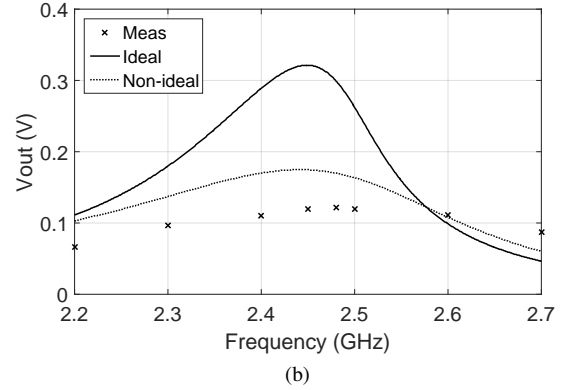
Fig. 11. (a) Circuit diagram of the hybrid RF solar harvester and (b) picture of the complete harvester prototype.

as shown in Fig. 3 (a). The equivalent circuit model of the solar cell was utilized to design the harvester circuit in ADS. To begin with, this work initially characterized the RF-dc conversion circuit independent from the solar cell.

The goal of the RF-dc conversion circuit design was to produce sufficient voltage and power to drive the PMU. Specifically, the bq25504 IC requires 330 mV and 15  $\mu$ W to start up from a “cold state”, and it can sustain operation for a minimum input voltage of 80 mV. Also, the IC has an integrated maximum power point tracking function which optimally adjusts the load resistance value for the maximum output power [45]. This work utilized a two diode RF rectifier



(a)

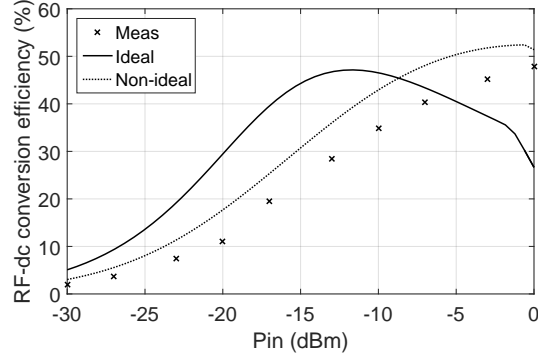


(b)

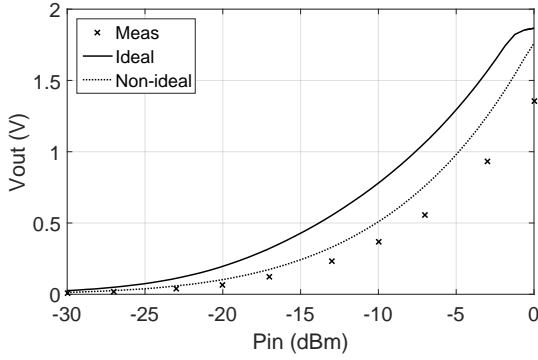
Fig. 12. Measured and simulated (a) RF-dc conversion efficiency and (b) dc output voltage with respect to frequency with optimal load resistance at -17 dBm RF input power.

(voltage doubler) circuit, which was necessary to accommodate a sufficiently high voltage to facilitate the start-up of the dc-dc converter circuit, as shown in Fig. 11 (a). To simplify the layout, the solar cell output was connected using a series diode at the output of the RF rectifier circuit as depicted in Fig. 11.

The matching circuit design was optimized to maximize the dc output power for a given RF available input power of -17 dBm. This is the minimum required RF input power to generate the minimum dc input voltage (80 mV) of the PMU in the “hot state”, according to preliminary simulations for different dc output current values from the solar cell, corresponding to different solar light irradiation conditions. Fig. 12 and Fig. 13 show the RF-dc conversion efficiency and the output voltage of the rectifier prototype without connecting a solar cell as a function of the frequency for an input RF power level of -17 dBm and as a function of the power level of the input (harvested) RF signals at the frequency of 2.45 GHz, respectively. In these figures, both “ideal” and “non-ideal” are simulation results with ADS. “Ideal” simulations use ideal lumped component models and “non-ideal” simulations use non-ideal lumped component models, provided by Johanson Technology for the components used in the prototype. For these measurements, RF power was measured using an RF power meter (NRP-Z211 from Rohde and Schwarz). The aggregate dc output power ( $P_{out}$ ) from the RF energy harvester and the solar cell was calculated using the following



(a)



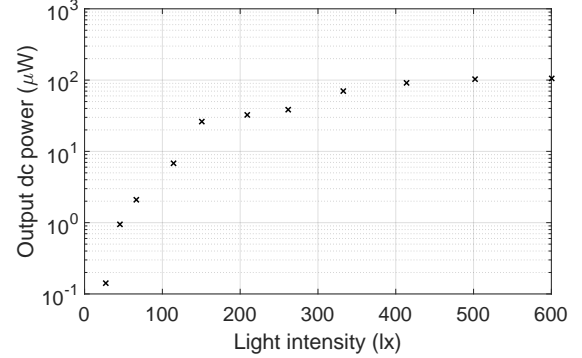
(b)

Fig. 13. Measured and simulated (a) RF-dc conversion efficiency and (b) dc output voltage with respect to input power with optimal load resistance at 2.45 GHz.

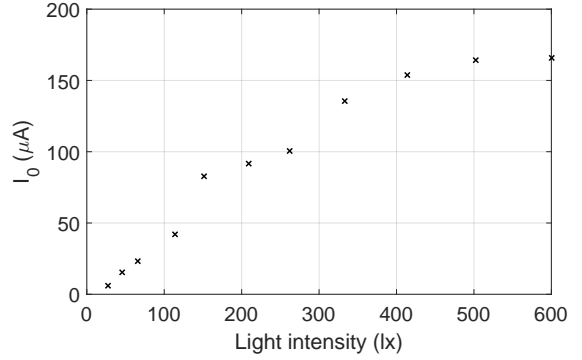
equation (1), where  $V_{out}$  is the measured output voltage and  $R_{load}$  is the load resistance. The RF energy harvester exhibits about 20 to 45 % RF-dc conversion efficiency depending on the RF input power in the range of -17 to 0 dBm.

$$P_{out} = \frac{V_{out}^2}{R_{load}} \quad (1)$$

Next, the performance of the RF-dc conversion circuit including the solar cell was characterized through simulations and measurements. Fig. 14 (a) and (b) depict the output power and the output current from the solar cell for the optimal load resistance of  $3.8 \text{ k}\Omega$  with reference to the ambient light intensity, respectively. The light intensity, measured utilizing a luminometer, was controlled by adjusting the distance between a table lamp and the solar cell. From these measurements, the solar cell yielded  $70.5 \mu\text{W}$  of output dc power and  $135.5 \mu\text{A}$  of output dc current at the room light condition of  $334 \text{ lx}$  irradiation. In addition, this work simulated the output power from the hybrid RF solar harvester with respect to the current from the solar cell ( $I_0$ ) for the RF power levels of -17 dBm and -10 dBm for the optimal load at 2.45 GHz as shown in Fig. 15. The simulation results confirm that the dc combination of the solar cell and the RF circuit exhibits a higher output dc power without affecting the performance of the RF-dc conversion circuit and the solar cell. However, if the solar energy is dominant, the performance of the solar cell slightly degrades. Finally, Fig. 16 shows the simulated and the measured  $S_{11}$  of



(a)



(b)

Fig. 14. Measured (a) output dc power and (b) dc current ( $I_0$ ) from the solar cell with respect to the light intensity for the load resistance of  $3.8 \text{ k}\Omega$ .

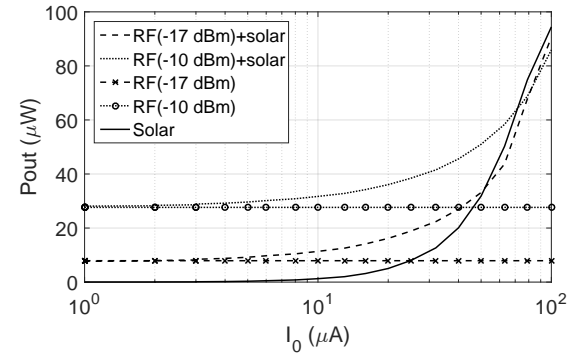


Fig. 15. Simulated output dc power with respect to the output dc current from the solar cell ( $I_0$ ) for RF input power of -17 dBm and -10 dBm.

the harvester for the input RF power of -17 dBm at 2.45 GHz when the input current from the solar cell is varied. The current from the solar cell was varied by changing the light intensity in the same manner as described above. The return loss ( $|S_{11}|$ ) increases first as  $I_0$  increases, but it decreases if the input current is too large and the solar power is dominant.

## V. MODULE-LEVEL OPERATION TEST

After optimizing the subsystems of the proposed hybrid harvester, a module-level operation test of the RF solar harvester utilizing a bq25504 module as a load resistance  $R_L$  in Fig. 11 (a) was performed to evaluate the capability of the harvester

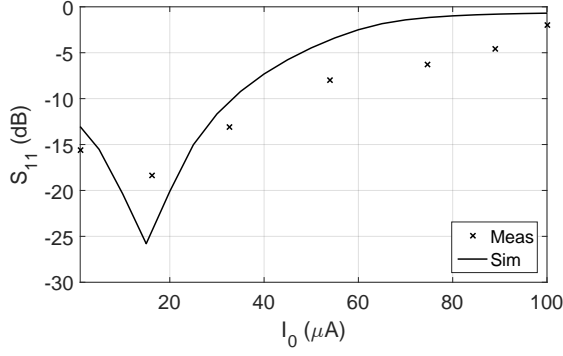


Fig. 16. Simulated and measured  $S_{11}$  with respect to output current from the solar cell ( $I_0$ ).

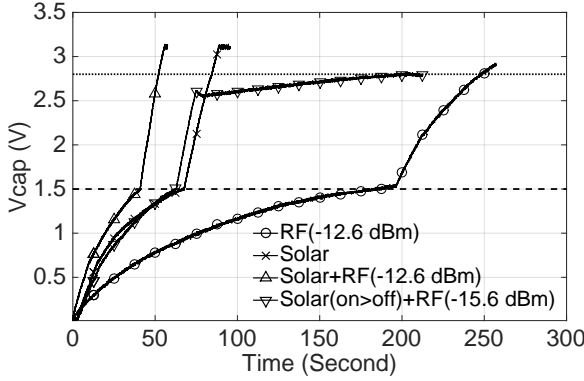


Fig. 17. Voltage in the  $100\mu\text{F}$  capacitor that is integrated in the bq25504 PMU during charging under different RF and solar conditions: (1) -12.6 dBm RF input power, (2) solar under room light condition, (3) -12.6 dBm RF input power + solar under room light condition, and (4) -15.6 dBm RF input power + solar under room light condition until cold start mode is over.

to “cold” start up the PMU. Fig. 17 shows the voltage of the  $100\mu\text{F}$  capacitor that is integrated in the bq25504 PMU during charging. The dashed line expresses the threshold of 1.5 V when the IC switches the operation mode from the cold start to the hot start. Similarly, the dotted line indicates the threshold of 2.8 V when VBAT\_OK signal, which is a

digital output for a battery good indicator, from the PMU is sufficiently high so that the capacitor voltage is adequate and the energy storage capacitor is ready to power the external dc load by turning on a MOSFET switch. The maximum output voltage is regulated at 3.3 V to protect a battery which can be externally connected, but this voltage can be arbitrary selected within the range of 2.4 to 5.3 V. The first three traces in Fig. 17 represent three different charging conditions: (1) -12.6 dBm RF input power, (2) solar cell at room light condition, and (3) aggregate dc combining the two harvesters, respectively. The input RF power of -12.6 dBm is the minimum required RF power to start the operation of bq25504 module from the “cold start” condition without using any solar cell. The comparison between (2) and (3) in Fig. 17 suggests that the charging time significantly decreases combining the dc output of the solar and the RF harvesters. More specifically, the time to charge the capacitor from 0 V to 2.8 V under the charging conditions (2) and (3) is 86 s and 51 s, respectively. Therefore, 40 % of capacitor charging time reduction is confirmed through the measurement. The last trace in Fig. 17 shows another charging condition (4) by combining the dc outputs of the solar and the RF harvester for the lower input power level of -15.6 dBm. In this trace, the change in slope around 2.5 V indicates that the light intensity was drastically reduced from 334 to 18.9 lx at this point by covering the solar cell. The input RF power of -15.6 dBm, which is the half of -12.6 dBm, cannot support alone the operation of the “cold start” operation mode. However, with the help of solar energy, this hybrid energy harvesting system can go over the “cold start” mode. For non-sufficient light irradiation conditions (e.g. in the night or in completely dark rooms), even a solar panel may not be used to “cold start” the system. However, once the IC starts operating with “hot start” mode after an initial relatively strong light irradiation, the input RF power of -15.6 dBm can maintain the perpetual operation of the IC, while the PMU gradually charges the capacitor using the ambient RF energy even under dark conditions.

TABLE III  
ENERGY HARVESTING SYSTEM PERFORMANCE COMPARISON

	Energy source	Antenna frequency	Maximum gain (dBi)	Polarization	Communication capability	Load	Sensitivity
This work	EM/Light	2.28 to 2.55 GHz	7.4	Circular	RF Transceiver (simultaneously with harvesting)	PMU (bq25504) MCU RF Transceiver Sensor	-15.6 dBm @ 2.8 V
Niotaki [24]	EM/Light	2.3 to 2.45 GHz	1.9	-	-	PMU (bq25504) Sensor (Simulation)	-
Georgiadis [25]	EM/Light	868 MHz (no measurement data)	-	Linear	RFID	Oscillator	9.3 dBm @ 1.7 V
De Donno [26]	EM/Light	855 to 880 MHz	1.85	Linear	-	MCU Dc-dc converter Sensor EEPROM	-14 dBm @ 2.4 V
Pinuela [9]	EM	470 to 2017 MHz (multiple antennas)	4.48 to 4.76	Linear	-	PMU (bq25504)	-25 dBm (single) -29 dBm (array) @ 2.4 to 5.3 V
Vyas [8]	EM	511 to 566 MHz (wideband)	7.3	Linear	-	MCU Sensor	-14.6 dBm @ 1.8 V

## VI. HYBRID HARVESTER SYSTEM PERFORMANCE BENCHMARKING

Recently, there have been various reported energy harvesting systems which utilize a PMU including a dc-dc converter to increase the sensitivity of the systems. Therefore, Table III summarizes the performance of recently reported EM/solar and EM energy harvesting system in terms of energy source, antenna operation frequency, maximum gain, antenna polarization, communication capability, dc load, and sensitivity, which is the minimum required RF power to satisfy the dc voltage and power requirements for their load. Compared with other EM/solar energy harvesters, the proposed design has the highest antenna operation bandwidth, highest gain, circular polarization, which is more suitable for ambient RF energy harvesting than linear polarization because of the unknown polarization of the harvested transmitting antennas, and simultaneous wireless communication capability while harvesting ambient energy. Regarding sensitivity, this work exhibits the lowest required RF input power among the EM/solar energy harvesters summarized in Table III. The sensitivity can be increased by improving the RF-dc conversion efficiency and further reducing the system power requirement. For example, Pinuela et al. have reported the lowest required RF input power of -29 dBm for the same bq25504 PMU [9] for the cold-start. Although, according to the datasheet of bq25504 PMU, this IC requires the minimum dc input power of 15  $\mu$ W for cold-start [45], which is more than 10 times higher than the reported sensitivity in [9] without considering RF-dc conversion loss that is typically more than 70 % of RF input power with input power below -20 dBm.

## VII. CONCLUSION

This paper investigates the potential of multiple energy harvesting system for the cold start and the subsequent perpetual operation of low profile the low power wireless sensor motes. This research effort demonstrated the design of a dual solar and electromagnetic energy harvesting and communication system which operates at 2.4 GHz ISM band enabling the operation of a low power PMU for a wireless sensor. The harvester consists of a dual-port rectangular slot antenna, a 3D printed package, a solar cell, an RF-dc converter, a PMU, an MCU, and an RF transceiver and every component was designed and characterized through simulation and measurements. As a result, this novel antenna with simultaneous harvesting and communication capabilities exhibited a performance satisfying the design goals of (1)  $S_{11}$  and  $S_{22}$  below -13 dB, (2)  $S_{21}$  below -13 dB, and (3) axial ratio below 3 dB in the frequency range of 2.4 to 2.5 GHz. Similarly, the designed miniaturized RF-dc conversion circuit generated sufficient voltage and power to support the operation of the bq25504 PMU from RF input power as low as -12.6 dBm and -15.6 dBm at the “cold start” and “hot start” condition, respectively. The module-level operation test of the PMU utilizing the hybrid RF/solar energy harvester confirmed a 40 % reduction in the capacitor charging time and a 50 % reduction in the minimum required RF input power compared to the independent operation of the RF and the solar harvester

under the room light irradiation condition of 334 lx. As a future work, all circuit components in Fig. 1 will be integrated to two printed circuit boards (PCBs), one for the antenna, communication, and rectification and another one for the power management and the micro-controller. Both of them are arranged in a printed 3D package which will have an opening to connect the micro-controller unit to a debugger to program the chip. We plan to connect the PCBs with a flexible ribbon cable in the package. The solar cell will be attached on the top of the communication/harvesting board. The MCU can be programmed for wireless measurement as reported in [15]. The proposed hybrid energy harvester could find numerous applications in IoT, smart skin and M2M applications in rugged operation conditions.

## VIII. ACKNOWLEDGMENT

We thank W. Chow, C. Fuentes-Hernandez, and B. Kippelen with Georgia Institute of Technology the School of Electrical and Computer Engineering for giving us precious advice about organic photovoltaic from the view point of their expertise.

## REFERENCES

- [1] H. Nishimoto, Y. Kawahara, and T. Asami, “Prototype implementation of ambient RF energy harvesting wireless sensor networks,” *2010 IEEE Sensors*, Nov 2010. [Online]. Available: <http://dx.doi.org/10.1109/ICSENS.2010.5690588>
- [2] L. Atzori, A. Iera, and G. Morabito, “The Internet of Things: A survey,” *Computer Networks*, vol. 54, no. 15, pp. 2787–2805, Oct 2010. [Online]. Available: <http://dx.doi.org/10.1016/j.comnet.2010.05.010>
- [3] L. Gao, Y. Zhang, V. Malyarchuk, L. Jia, K.-I. Jang, R. Chad Webb, H. Fu, Y. Shi, G. Zhou, L. Shi, and et al., “Epidermal photonic devices for quantitative imaging of temperature and thermal transport characteristics of the skin,” *Nature Communications*, vol. 5, p. 4938, Sep 2014. [Online]. Available: <http://dx.doi.org/10.1038/ncomms5938>
- [4] B. S. Cook, T. Le, S. Palacios, A. Traill, and M. Tentzeris, “Only skin deep: Inkjet-printed zero-power sensors for large-scale RFID-integrated smart skins,” *IEEE Microw. Mag.*, vol. 14, no. 3, pp. 103–114, 2013. [Online]. Available: <http://dx.doi.org/10.1109/MMM.2013.2240855>
- [5] S. Kim, R. Vyas, J. Bito, K. Niotaki, A. Collado, A. Georgiadis, and M. Tentzeris, “Ambient RF Energy-Harvesting Technologies for Self-Sustainable Standalone Wireless Sensor Platforms,” *Proc. IEEE*, vol. 102, no. 11, pp. 1649–1666, Nov. 2014.
- [6] S. Priya and D. J. Inman, *Energy harvesting technologies*. Springer, 2009, vol. 21.
- [7] J. A. Paradiso and T. Starner, “Energy scavenging for mobile and wireless electronics,” *IEEE Pervasive Comput.*, vol. 4, no. 1, pp. 18–27, Jan. 2005.
- [8] R. J. Vyas, B. B. Cook, Y. Kawahara, and M. M. Tentzeris, “E-WEHP: A Batteryless Embedded Sensor-Platform Wirelessly Powered From Ambient Digital-TV Signals,” *IEEE Trans. Microw. Theory Tech.*, vol. 61, no. 6, pp. 2491–2505, Jun. 2013.
- [9] M. Pinuela, P. D. Mitcheson, and S. Lucyszyn, “Ambient RF Energy Harvesting in Urban and Semi-Urban Environments,” *IEEE Trans. Microw. Theory Tech.*, vol. 61, no. 7, pp. 2715–2726, Jul. 2013.
- [10] C. R. Valenta and G. D. Durgin, “Harvesting Wireless Power: Survey of Energy-Harvester Conversion Efficiency in Far-Field, Wireless Power Transfer Systems,” *IEEE Microw. Mag.*, vol. 15, no. 4, pp. 108–120, June 2014.
- [11] X. Lu, P. Wang, D. Niyato, D. I. Kim, and Z. Han, “Wireless Networks with RF Energy Harvesting: A Contemporary Survey,” *IEEE Commun. Surveys Tuts.*, vol. 17, no. 2, pp. 757–789, 2015.
- [12] K. Gudun, S. Shao, J. J. Hull, A. Hoang, J. Ensworth, and M. S. Reynolds, “Ultra-low power autonomous 2.4GHz RF energy harvesting and storage system,” in *2015 IEEE Int. Conf. on RFID-TA*, Tokyo, Japan, Sep 2015.
- [13] W. S. Wong, M. L. Chabinyc, T.-N. Ng, and A. Salleo, “Materials and novel patterning methods for flexible electronics,” *Electron. Materials: Science and Tech.*, pp. 143–181, 2009.

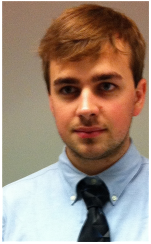
- [14] L. Yang, A. Rida, R. Vyas, and M. M. Tentzeris, "RFID Tag and RF structures on a Paper Substrate Using Inkjet-Printing Technology," *IEEE Trans. Microw. Theory Tech.*, vol. 55, no. 12, pp. 2894–2901, Dec. 2007.
- [15] J. Bito, J. G. Hester, and M. M. Tentzeris, "Ambient RF Energy Harvesting From a Two-Way Talk Radio for Flexible Wearable Wireless Sensor Devices Utilizing Inkjet Printing Technologies," *IEEE Trans. Microw. Theory Tech.*, vol. 63, no. 12, pp. 4533–4543, Dec 2015.
- [16] J. G. Hester, S. Kim, J. Bito, T. Le, J. Kimionis, D. Revier, C. Saintsing, S. Wenjing, B. Tehrani, A. Traille, B. S. Cook, and M. M. Tentzeris, "Additively Manufactured Nanotechnology and Origami-Enabled Flexible Microwave Electronics," *Proc. IEEE*, vol. 103, no. 4, pp. 583–606, Apr. 2015.
- [17] B. Tehrani, B. Cook, J. Cooper, and M. Tentzeris, "Inkjet printing of a wideband, high gain mm-Wave Vivaldi antenna on a flexible organic substrate," in *2014 IEEE Antennas and Propag. Society Int. Symp.*, Memphis, TN, USA, Jul 2014.
- [18] J. Bito, B. Tehrani, B. Cook, and M. Tentzeris, "Fully inkjet-printed multilayer microstrip patch antenna for Ku-band applications," in *2014 IEEE Antennas and Propag. Society Int. Symp.*, Memphis, TN, USA, July. 2014, pp. 854–855.
- [19] B. S. Cook, J. R. Cooper, and M. M. Tentzeris, "Multi-Layer RF Capacitors on Flexible Substrates Utilizing Inkjet Printed Dielectric Polymers," *IEEE Microw. Wireless Compon. Lett.*, vol. 23, no. 7, pp. 353–355, Jul. 2013.
- [20] B. S. Cook, C. Mariotti, J. R. Cooper, D. Revier, B. K. Tehrani, L. Aluigi, L. Roselli, and M. M. Tentzeris, "Inkjet-printed, vertically-integrated, high-performance inductors and transformers on flexible LCP substrate," in *2014 IEEE MTT-S Int. Microwave Symp. Dig.*, Tampa, FL, USA, Jun. 2014, pp. 1–4.
- [21] N. Sani, M. Robertsson, P. Cooper, X. Wang, M. Svensson, P. Andersson Ersman, P. Norberg, M. Nilsson, D. Nilsson, X. Liu, H. Hesselbom, L. Akesso, M. Fahlman, X. Crispin, I. Engquist, M. Berggren, and G. Gustafsson, "All-printed diode operating at 1.6 GHz," *Proc. of the Nat. Academy of Sciences*, vol. 111, no. 33, pp. 11943–11948, 2014.
- [22] P. I. Deffenbaugh, R. C. Rumpf, and K. H. Church, "Broadband microwave frequency characterization of 3-D printed materials," *IEEE Trans. Compon. Packag. Technol.*, vol. 3, no. 12, pp. 2147–2155, Dec 2013. [Online]. Available: <http://dx.doi.org/10.1109/TCPMT.2013.2273306>
- [23] S. Zhang, C. C. Njoku, W. G. Whittow, and J. C. Vardaxoglou, "Novel 3D printed synthetic dielectric substrates," *Microwave and Optical Technology Letters*, vol. 57, no. 10, pp. 2344–2346, Jul 2015. [Online]. Available: <http://dx.doi.org/10.1002/mop.29324>
- [24] K. Niotaki, F. Giuppi, A. Georgiadis, and A. Collado, "Solar/EM energy harvester for autonomous operation of a monitoring sensor platform," *Wireless Power Transfer*, vol. 1, no. 01, pp. 44–50, Mar 2014.
- [25] A. Georgiadis and A. Collado, "Improving range of passive RFID tags utilizing energy harvesting and high efficiency class-E oscillators," *2012 6th European Conference on Antennas and Propagation (EuCAP)*, Mar 2012. [Online]. Available: <http://dx.doi.org/10.1109/EuCAP.2012.6206429>
- [26] D. De Donno, L. Catarinucci, and L. Tarricone, "An UHF RFID energy-harvesting system enhanced by a DC-dc charge pump in silicon-on-insulator technology," *IEEE Microw. Wireless Compon. Lett.*, vol. 23, no. 6, pp. 315–317, Jun 2013. [Online]. Available: <http://dx.doi.org/10.1109/LMWC.2013.2258002>
- [27] Y. Zhou, T. M. Khan, J. W. Shim, A. Dindar, C. Fuentes-Hernandez, and B. Kippelen, "All-plastic solar cells with a high photovoltaic dynamic range," *J. of Materials Chemistry A*, vol. 2, no. 10, p. 3492, 2014.
- [28] J. Tong, S. Xiong, Y. Zhou, L. Mao, X. Min, Z. Li, F. Jiang, W. Meng, F. Qin, T. Liu, and et al., "Flexible all-solution-processed all-plastic multijunction solar cells for powering electronic devices," *Mater. Horiz.*, vol. 3, no. 5, pp. 452–459, 2016.
- [29] T. M. Eggenhuisen, Y. Galagan, A. F. K. V. Biezemans, T. M. W. L. Slaats, W. Voorthuizen, S. Kommeren, S. Shanmugam, J. Teunissen, A. Hadipour, W. J. H. Verhees, S. C. Veenstra, M. J. J. Coenen, J. Gilot, R. Andriessen, and W. A. Groen, "High efficiency, fully inkjet printed organic solar cells with freedom of design," *J. of Materials Chemistry A*, vol. 3, no. 14, pp. 7255–7262, 2015.
- [30] M. Danesh and J. R. Long, "Photovoltaic Antennas for Autonomous Wireless Systems," *IEEE Trans. Circuits Syst. II*, vol. 58, no. 12, pp. 807–811, Dec 2011.
- [31] A. Collado and A. Georgiadis, "Conformal Hybrid Solar and Electromagnetic (EM) Energy Harvesting Rectenna," *IEEE Trans. Circuits Syst. I*, vol. 60, no. 8, pp. 2225–2234, Aug 2013.
- [32] K. Niotaki, A. Georgiadis, and A. Collado, "Dual-band rectifier based on resistance compression networks," in *2014 IEEE MTT-S Int. Microwave Symp. Dig.*, Tampa, FL, USA, Jun. 2014, pp. 1–3.
- [33] S. Hemour and K. Wu, "Radio-Frequency Rectifier for Electromagnetic Energy Harvesting: Development Path and Future Outlook," *Proc. IEEE*, vol. 102, no. 11, pp. 1667–1691, Nov 2014.
- [34] C. H. P. Lorenz, S. Hemour, W. Li, Y. Xie, J. Gauthier, P. Fay, and K. Wu, "Overcoming the efficiency limitation of low microwave power harvesting with backward tunnel diodes," in *2015 IEEE MTT-S Int. Microwave Symp. Dig.*, Phoenix, AZ, USA, May 2015, pp. 1–4.
- [35] K. Niotaki, S. Kim, S. Jeong, A. Collado, A. Georgiadis, and M. M. Tentzeris, "A Compact Dual-Band Rectenna Using Slot-Loaded Dual Band Folded Dipole Antenna," *IEEE Antennas Wireless Propag. Lett.*, vol. 12, pp. 1634–1637, 2013. [Online]. Available: <http://dx.doi.org/10.1109/LAWP.2013.2294200>
- [36] H. Sun, Y.-x. Guo, M. He, and Z. Zhong, "A Dual-Band Rectenna Using Broadband Yagi Antenna Array for Ambient RF Power Harvesting," *IEEE Antennas Wireless Propag. Lett.*, vol. 12, pp. 918–921, July 2013.
- [37] F. Bolos, D. Belo, and A. Georgiadis, "A UHF rectifier with one octave bandwidth based on a non-uniform transmission line." San Francisco, CA, USA: Institute of Electrical and Electronics Engineers (IEEE), May 2016. [Online]. Available: <http://dx.doi.org/10.1109/MWSYM.2016.7540083>
- [38] A. Wang, B. H. Calhoun, and A. P. Chandrakasan, *Sub-threshold design for ultra low-power systems*. Springer, 2006, vol. 95.
- [39] A. Bryant, J. Brown, P. Cottrell, M. Ketchen, J. Ellis-Monaghan, and E. Nowak, "Low-power CMOS at V<sub>dd</sub>=4kT/q," *Device Research Conf.*, Jun 2001. [Online]. Available: <http://dx.doi.org/10.1109/DRC.2001.937856>
- [40] M. Vieira, C. Coelho, D. da Silva, and J. da Mata, "Survey on wireless sensor network devices," *IEEE Conf. on Emerging Technologies and Factory Automation*, 2003. [Online]. Available: <http://dx.doi.org/10.1109/ETFA.2003.1247753>
- [41] Texas Instruments, "MSP430F22x4: MIXED SIGNAL MICROCONTROLLER," Aug. 2012.
- [42] K. Gudan, S. Shao, J. J. Hull, J. Ensworth, and M. S. Reynolds, "Ultra-low power 2.4GHz RF energy harvesting and storage system with -25dBm sensitivity," in *2015 IEEE Int. Conf. on RFID*, San Diego, CA, USA, Apr 2015.
- [43] E. J. Carlson, K. Strunz, and B. P. Otis, "A 20 mV Input Boost Converter with Efficient Digital Control for Thermoelectric Energy Harvesting," *IEEE J. Solid-State Circuits*, vol. 45, no. 4, pp. 741–750, Apr 2010.
- [44] S.-E. Adami, V. Marian, N. Degrenne, C. Vollaie, B. Allard, and F. Costa, "Self-powered ultra-low power DC-DC converter for RF energy harvesting," in *2012 IEEE FTFC*, Paris, France, Jun 2012.
- [45] Texas Instruments, "bq25504-Ultra Low Power Boost Converter with Battery Management for Energy Harvester Applications," Oct. 2012.
- [46] —, "CC2500: Low-Cost Low-Power 2.4 GHz RF Transceiver," 2010.
- [47] S. Shi, K. Hirasawa, and Z. N. Chen, "Circularly polarized rectangularly bent slot antennas backed by a rectangular cavity," *IEEE Trans. Antennas Propag.*, vol. 49, no. 11, pp. 1517–1524, Nov 2001.
- [48] R. Li, B. Pan, A. N. Traille, J. Papapolymerou, J. Laskar, and M. M. Tentzeris, "Development of a Cavity-Backed Broadband Circularly Polarized Slot/Strip Loop Antenna With a Simple Feeding Structure," *IEEE Trans. Antennas Propag.*, vol. 56, no. 2, pp. 312–318, 2008. [Online]. Available: <http://dx.doi.org/10.1109/TAP.2007.915412>
- [49] T. Nakatsuka, "Polylactic acid-coated cable," *Fujikura Tech. Rev.*, vol. 3946, no. 7, 2011.
- [50] V. V. Meriakri, D. S. Kalenov, M. P. Parkhomenko, S. Zhou, and N. A. Fedoseev, "Dielectric properties of biocompatible and biodegradable polycaprolone and polylactide and their nanocomposites in the millimeter wave band," *American J. of Materials Science*, vol. 2, no. 6, pp. 171–175, Jan 2013.



**Jo Bito** (S'13) received the B.S. in electrical and electronic engineering from Okayama University, Okayama, Japan in 2013. From 2010 to 2011, he joined the international programs in engineering (IPENG), and studied at University of Illinois Urbana-Champaign, Champaign, IL, USA. He received the M.S. in electrical and computer engineering from the Georgia Institute of Technology, Atlanta, in 2016 where he is now pursuing his Ph.D degree, as a research assistant in the Agile Technologies for High-performance Electromagnetic

Novel Applications (ATHENA) Group.

His research interests include the application of inkjet printing technology for flexible and wearable electronics, RF energy harvesting, and wireless power transfer systems. He was a recipient of the Japan Student Services Organization (JASSO) Long Term Scholarship beginning in 2013.



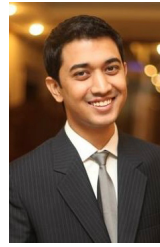
**Ryan Bahr** (S'11) received the B.S. and M.S degree in electrical engineering from the Georgia Institute of Technology, Atlanta, GA. He is currently working on the Ph.D. degree in electrical and computer engineering from the Georgia Institute of Technology, where he is supervised by Prof. Tentzeris. His research focuses on applying 3D printing techniques for millimeter wave and packaging applications utilizing new materials.



**Jimmy G. Hester** (S'14) spent two intense preparation years studying fundamental chemistry, math and physics after which he was admitted in INP Toulouse, ENSEEIHT where he received a graduate degree and M.S degree in electrical and signal processing engineering, majoring in radio frequency electronics, in 2012 and 2014, respectively. He received the M.S. in electrical and computer engineering from the Georgia Institute of Technology, Atlanta, in 2014 where he is now working, as a research assistant in the ATHENA group, towards

his PhD degree in Electrical and Computer Engineering.

His research interests lie at the interface between radio frequency engineering and material science, in the form of flexible electronics technologies and nanotechnologies. Recently, he has been working towards the use of carbon nanomaterials applied to inkjet-printed RF sensing components for flexible low cost ubiquitous gas sensing applications. His work covers the entire development process, from the development of inkjet inks, improvement of fabrication methods, sensor component design, high frequency characterization and environmental testing to the design, simulation and fabrication of the RF system embedding the sensor.



**Syed Abdullah Nauroze** (S'13) received his B.Sc. (honors) in computer engineering from University of Engineering and Technology, Taxila Pakistan in 2005 and M.Sc. in electrical engineering from Royal Institute of Technology (KTH), Stockholm, Sweden in 2008. During 2008-09 he worked at Microsystems Technology Laboratory (KTH), where he conducted research on on-chip millimeter-wave antennas for automotive radar and future wireless applications. He is currently pursuing his Ph.D. in electrical and computer engineering at Georgia Institute of

Technology, Atlanta, USA where he is working as a Research Assistant at ATHENA lab. Mr. Nauroze has a teaching experience of seven (7) years.

His research interests include application of additive manufacturing techniques like 3D printing and ink-jet printing for flexible and origami-based RF structures. He is also a recipient of prestigious Swedish Institute scholarship in 2006 and Fulbright Scholarship in 2014 for his masters and Ph. D. degrees respectively.



**Apostolos Georgiadis** (S'94-M'02-SM'08) was born in Thessaloniki, Greece. He received the B.S. degree in physics and the M.S. degree in telecommunications from the Aristotle University of Thessaloniki, Greece, in 1993 and 1996, respectively. He received the Ph.D. degree in electrical engineering from the University of Massachusetts, Amherst, in 2002. In 1995, he spent a semester with Radio Antenna Communications (R.A.C.), Milan Italy, working on Yagi antennas for U.H.F. applications.

In 2000, he spent three months with Telaxis Communications, South Deerfield MA USA, assisting in the design and testing of a pillbox antenna for LMDS applications. In 2002 he joined Global Communications Devices (GCD), North Andover MA USA, as a Systems Engineer and worked on CMOS transceivers for wireless network applications. In June 2003, he joined Bermai, Inc., Minnetonka MN USA, as an RF/Analog Systems Architect. In 2005 he joined the University of Cantabria, Spain, as a Juan de la Cierva Fellow researcher. In 2006 he was a consultant for Bitwave Semiconductor, Lowell MA, US. In addition he collaborated with ACORDE S.A., Santander, Spain, in the design of integrated CMOS VCOs for ultra-wideband (UWB) applications. In March 2007, he joined CTTC, Spain as a senior researcher in communications subsystems. In 2013-2016 he was group leader of the Microwave Systems and Nanotechnology Department at CTTC. In July 2016, he joined Heriot-Watt University, Edinburgh as an Associate Professor.

In 1996, Dr. Georgiadis received a Fulbright Scholarship for graduate studies at the University of Massachusetts, Amherst. He received the Outstanding Teaching Assistant Award from the University of Massachusetts, Amherst, in 1997 and 1998. He also was the recipient of the Eugene M. Isenberg Award from the Isenberg School of Management, University of Massachusetts, Amherst, in 1999 and 2000. He was the General Chair of 2011 IEEE RFID-TA Conference and general co-Chair of the 2011 IEEE MTT-S IMWS on Millimeter Wave Integration Technologies. He was the Chairman of EU COST Action IC0803 RF/Microwave communication subsystems for emerging wireless technologies (RFCSET) and he is presently Vice-Chair of EU COST Action IC1301 Wireless Power Transmission for Sustainable Electronics (WiPE). He was the Coordinator of Marie Curie Industry-Academia Pathways and Partnerships (IAPP) project Symbiotic Wireless Autonomous Powered system (SWAP). He is a EU Marie Curie Global Fellow. He is Member of the IEEE MTT-S TC-24 RFID Technologies (past Chair) and Member of IEEE MTT-S TC-26 Wireless Energy Transfer and Conversion. He serves as an Associate Editor of the IEEE Journal on RFID. He was Associate Editor of the IET Microwaves Antennas and Propagation Journals, IEEE Microwave and Wireless Components Letters and the IEEE RFID Virtual Journal. He is founder and Editor-in-Chief of the Cambridge Wireless Power Transfer Journal. He is Vice Chair of URSI Commission D, Electronics and Photonics and ADCOM Member of IEEE Council on RFID serving as Vice President of Conferences. He is a Distinguished Lecturer of IEEE Council on RFID. He received the 3rd place 2016 Bell Labs Award.

His research interests include energy harvesting and wireless power transmission, RFID technology, active antennas and phased array antennas, inkjet and 3D printed electronics, millimeter wave systems. He has published more than 150 papers in peer reviewed journals and international conferences.



**Manos M. Tentzeris** (S'89-M'92-SM'03-F'10) Professor Manos M. Tentzeris received the Diploma Degree in Electrical and Computer Engineering from the National Technical University of Athens ("Magna Cum Laude") in Greece and the M.S. and Ph.D. degrees in Electrical Engineering and Computer Science from the University of Michigan, Ann Arbor, MI and he is currently Ken Byers Professor in Flexible Electronics with School of ECE, Georgia Tech, Atlanta, GA. He has published more than 620 papers in refereed Journals and

Conference Proceedings, 5 books and 25 book chapters. Dr. Tentzeris has helped develop academic programs in 3D/inkjet-printed RF electronics and modules, flexible electronics, origami and morphing electromagnetics, Highly Integrated/Multilayer Packaging for RF and Wireless Applications using ceramic and organic flexible materials, paper-based RFID's and sensors, wireless sensors and biosensors, wearable electronics, "Green" electronics, energy harvesting and wireless power transfer, nanotechnology applications in RF, Microwave MEM's, SOP-integrated (UWB, multiband, mmW, conformal) antennas and heads the ATHENA research group (20 researchers). He has served as the Head of the GT-ECE Electromagnetics Technical Interest Group, as the Georgia Electronic Design Center Associate Director for RFID/Sensors research and as the Georgia Tech NSF-Packaging Research Center Associate Director for RF Research and the RF Alliance Leader.

He was the recipient/co-recipient of the 2015 IET Microwaves, Antennas and Propagation Premium Award, the 2014 Georgia Tech ECE Distinguished Faculty Achievement Award, the 2014 IEEE RFID-TA Best Student Paper Award, the 2013 IET Microwaves, Antennas and Propagation Premium Award, the 2012 FiDiPro Award in Finland, the iCMG Architecture Award of Excellence, the 2010 IEEE Antennas and Propagation Society Piergiorgio L. E. Uslenghi Letters Prize Paper Award, the 2011 International Workshop on Structural Health Monitoring Best Student Paper Award, the 2010 Georgia Tech Senior Faculty Outstanding Undergraduate Research Mentor Award, the 2009 IEEE Transactions on Components and Packaging Technologies Best Paper Award, the 2009 E.T.S. Walton Award from the Irish Science Foundation, the 2007 IEEE APS Symposium Best Student Paper Award, the 2007 IEEE IMS Third Best Student Paper Award, the 2007 ISAP 2007 Poster Presentation Award, the 2006 IEEE MTT Outstanding Young Engineer Award, the 2006 Asian-Pacific Microwave Conference Award, the 2004 IEEE Transactions on Advanced Packaging Commendable Paper Award, the 2003 NASA Godfrey "Art" Anzic Collaborative Distinguished Publication Award, the 2003 IBC International Educator of the Year Award, the 2003 IEEE CPMT Outstanding Young Engineer Award, the 2002 International Conference on Microwave and Millimeter-Wave Technology Best Paper Award (Beijing, CHINA), the 2002 Georgia Tech-ECE Outstanding Junior Faculty Award, the 2001 ACES Conference Best Paper Award and the 2000 NSF CAREER Award and the 1997 Best Paper Award of the International Hybrid Microelectronics and Packaging Society. He was the TPC Chair for IEEE IMS 2008 Symposium and the Chair of the 2005 IEEE CEM-TD Workshop and he is the Vice-Chair of the RF Technical Committee (TC16) of the IEEE CPMT Society. He is the founder and chair of the RFID Technical Committee (TC24) of the IEEE MTT Society and the Secretary/Treasurer of the IEEE C-RFID. He is the Associate Editor of IEEE Transactions on Microwave Theory and Techniques, IEEE Transactions on Advanced Packaging and International Journal on Antennas and Propagation. Dr. Tentzeris was a Visiting Professor with the Technical University of Munich, Germany for the summer of 2002, a Visiting Professor with GTRI-Ireland in Athlone, Ireland for the summer of 2009 and a Visiting Professor with LAAS-CNRS in Toulouse, France for the summer of 2010. He has given more than 100 invited talks to various universities and companies all over the world. He is a Fellow of IEEE, a member of URSI-Commission D, a member of MTT-15 committee, an Associate Member of EuMA, a Fellow of the Electromagnetic Academy and a member of the Technical Chamber of Greece. Prof. Tentzeris served as one of the IEEE MTT-S Distinguished Microwave Lecturers from 2010-2012 and he is one of the IEEE CRFID Distinguished Lecturers.